Fibers and Polymers 2017, Vol.18, No.7, 1250-1254
DOI 10.1007/s12221-017-6814-7

ISSN 1229-9197 (print version)
ISSN 1875-0052 (electronic version)

PVDF/Cu-BTC Composite Membranes for Dye Separation

Yingbo Chen[1]*, Huiqiang Liu[1], Xiaoyu Hu[2], Bowen Cheng[3], Dongqing Liu[1], Yufeng Zhang[1], and Sankar Nair[1,4]

[1]*School of Materials Science and Engineering, State Key Laboratory of Separation Membranes and Membrane Processes, Tianjin Polytechnic University, Tianjin 300387, P. R. China*
[2]*State Key Laboratory of Membrane Materials and Membrane Applications, Tianjin Motimo Membrane Technology Co. Ltd., Tianjin 300042, P. R. China*
[3]*School of Textile, Tianjin Polytechnic University, Tianjin 300387, P. R. China*
[4]*School of Chemical and Biomolecular Engineering, Georgia Institute of Technology, Atlanta 30332, USA*
(Received August 10, 2016; Revised February 27, 2017; Accepted May 2, 2017)

Abstract: Membranes with high water permeation capability as well as high rejection to dye molecules are very important for dye separation. In this study, a metal organic framework structure (Cu-BTC) was fabricated *in situ* on a poly(vinyl difluoride) hollow fiber support for nanofiltration of dye solution. In order to protect the Cu-BTC layer, the surface was coated by crosslinking polyvinyl alcohol. The composite membranes showed no rejection to divalent salts and high rejection to Congo Red dye. It was noticed that several Cu-BTC layers could enhance dye rejection of the composite membranes. This novel composite membrane showed promising applications in the separation of dye molecules from aqueous solutions containing dissolved salts.

Keywords: Nanofiltration, MOFs, Dye separation, Composite membrane

Introduction

In the dye processing industry, a large amount of waste water is produced during the concentration of dye powders [1]. Dyes and salts are the main components in waste water, which needs to be treated by effective techniques. Among all treatment methods, membrane technology is a popular alternative for its high efficiency, low cost, and the fact that it is environmentally friendly [2-4]. Nanofiltration membrane is especially popular, which can retain organic molecules with molecular weights ranging from 200 to 1000 g/mol, and has been applied for dye separation [5]. For example, Banerjee *et al.* [6] removed dye from salt containing solution using nanofiltration in combination with an oxidation process. Fang *et al.* [7] used poly(vinyl chloride) grafted polymers as a nanofiltration membrane for dye separation. Maurya *et al.* [8] treated an aqueous dye solution using polyamide thin film composite hollow fiber nanofiltration membranes.

Although the latter two examples used single membranes to concentrate dye solutions, it has been observed that highly purified dyes cannot be obtained through membrane processes due to the rejection to salts from the membrane. The products contained both the dyes and the salts, especially in the case of divalent salts, such as sodium sulfate. Therefore, membranes with low or no rejection to salts but high rejection to dye molecules are the optimal choice for dye separation. Li *et al.* [9] used poly(vinyl difluoride) (PVDF) as a support membrane, coated with polyvinyl alcohol (PVA) and titanium dioxide nanoparticles to prepare nanofiltration membranes for dye desalination. The coated crosslinking PVA membranes showed no rejection to all monovalent and divalent salts present, but high rejection to dyes, such as Congo Red and methyl blue. However, the membrane prepared showed low water permeation due to the thick coating layer and thus high separation resistance.

Porous materials, such as zeolites [10], activated carbon [11], and metal-organic frameworks (MOFs) [12-14], have shown excellent performance in dye separation. However, in most cases the dye separation and removal are based on dye adsorption. Regeneration is needed for the reuse of the porous materials in order to release the dye molecules. Also, selectivity varies depending on the dyes, usually being limited, and it is hard to remove dyes by adsorption in solutions with high ionic strength.

In this study, we aimed to separate dyes from a salt containing solution by dye rejection and selective permeation of ions and water from MOFs. A novel composite membrane was fabricated by *in situ* formation of Cu-BTC on PVDF support membranes by immersing the membrane in MOF precursor solutions. The porous inorganic MOF layer separated the dye and salts; while the organic PVDF support hollow fiber membrane showed good mechanical properties for the composite membranes. The membrane structure and morphology were characterized using scanning electron microscopy (SEM), fourier transform infrared spectroscopy (FTIR), and X-ray diffraction (XRD). The performance of the membrane for dye separation was measured using Congo Red as a model dye molecule.

*Corresponding author: chenyingbo@tjpu.edu.cn

Experimental

Materials

Copper acetate ($Cu(CH_3COO)_2$, 99 %) was purchased from Tianjin Guangfu Fine Chemical Research Institute; trimesic acid (H_3BTC, 98 %) was purchased from Aladdin Reagent Co. Ltd.; the PVDF support membrane (average pore size 0.4 μm, pure water flux 150±14 $l m^{-2} h^{-1} bar^{-1}$) was supplied by Tianjin Motimo Co. Ltd.; PVA with an average molecular weight of 71,000 g/mol and glutaraldehyde (GA) were purchased from Tianjin Kermel Chemical reagent Co. Ltd. Congo Red and ethanol were purchased from Tianjin Kermel Chemical reagent Co. Ltd.

Membrane Preparation

The PVDF support membrane was immersed in pure water for two days and air dried. The membrane was then immersed in a 40 g/*l* $Cu(CH_3COO)_2$ aqueous solution for 1 h at room temperature and later air dried. It was then transferred to a 10 g/*l* H_3BTC-ethanol solution and kept at 60 °C for 24 h to obtain the PVDF/Cu-BTC membrane. In order to obtain the optimum amount of Cu-BTC on the membrane surface (PVDF/Cu-BTC/2 membrane), the above-described operation was repeated twice. To protect the Cu-BTC from degradation, a PVA layer was added on the Cu-BTC layer by immersing it in a 1 wt% PVA aqueous solution for 20 min, followed by crosslinking in 3 % glutaraldehyde for 20 min. A PVDF/PVA membrane was fabricated to be used as a comparison by immersing the PVDF membrane in a PVA solution using the similar method.

Membrane Characterization

All membranes were pre-treated in liquid nitrogen to create a clear cross sectional morphology for microscope observation. After sputtering gold on the surface, the membranes were examined by using a field emission scanning electron microscope (FESEM, S-4800, Japan, Hitachi) and an environmental scanning electron microscope (ESEM, Quanta-200, Czech, FEI). The infra-red (IR) spectra of the membranes were recorded using a TENSOR37 Bruker (German) FTIR spectrometer with 32 scans, a resolution of 4 cm^{-1}, and a range of 400-2000 cm^{-1}. X-ray diffraction (XRD) analysis was conducted using an X-ray diffractometer (Bruker AXS, German) with Cu target, an X-ray wavelength of 0.15402 nm, a scanning angle of 5-40 °, a voltage of 40 kV, and a current of 100 mA.

Membrane Performance Test

Membrane performance was analyzed by a cross-flow batch. The feed solution (50 mg/*l* Congo Red) was pumped to the membrane module at 0.5 MPa. The permeate was collected for 60 min and the permeate flux was calculated using equation (1).

$$F = \frac{V}{St} \tag{1}$$

where F is the permeate flux, S is the effective membrane area, V is the total volume of the permeate, and t is the filtration time. Rejection (R) was calculated using equation (2):

$$R = \left(1 - \frac{C_p}{C_f}\right) \times 100\% \tag{2}$$

where C_p and C_f are the concentration of the permeate and the feed solution, respectively. The reported flux and rejection values were the average of three measurements. The dye concentration was measured by a UV-vis spectrophotometer. Stability of the membranes was tested continuously for 3 days, being used for 4 h per day and kept in pure water between each test.

Results and Discussion

Membrane Characterization

Figure 1 shows the color change observed for the membranes. The PVDF support membrane and PVA coated membrane were white, while the PVDF/Cu-BTC membrane became blue due to the formation of Cu-BTC.

Figure 2 shows the SEM images of the membranes; a porous structure can be seen in the cross section and the surface of the PVDF membrane (Figure 2(a) & (e)). The needle-like pores found on the surface of the PVDF membrane were due to stretching during fabrication by a melting spinning process. The presence of a PVA layer covered the surface pores (Figure 2(b) & (f)) and thus the membrane could be used for nanofiltration [9]. MOF can be deposited on a polymeric membrane surface via in situ crystallization. It can be seen in Figure 2(c) & (g), after one reaction, some Cu-BTC crystals were formed on the surface, which was not fully covered. After a second reaction Cu-BTC crystals were formed and all pores were covered (Figure 2(d) & (h)). The thickness of the Cu-BTC layer measured from the SEM images was about 2.3 μm.

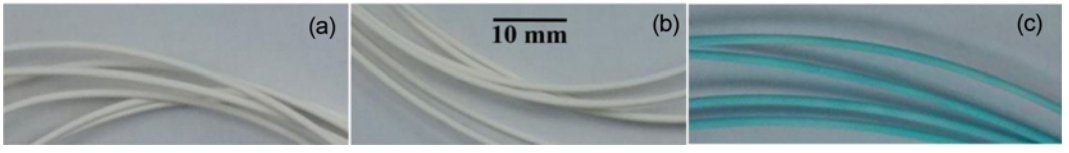

Figure 1. Photos of PVDF support membrane (a), PVA coated membrane (b), and PVDF/Cu-BTC membrane (c).

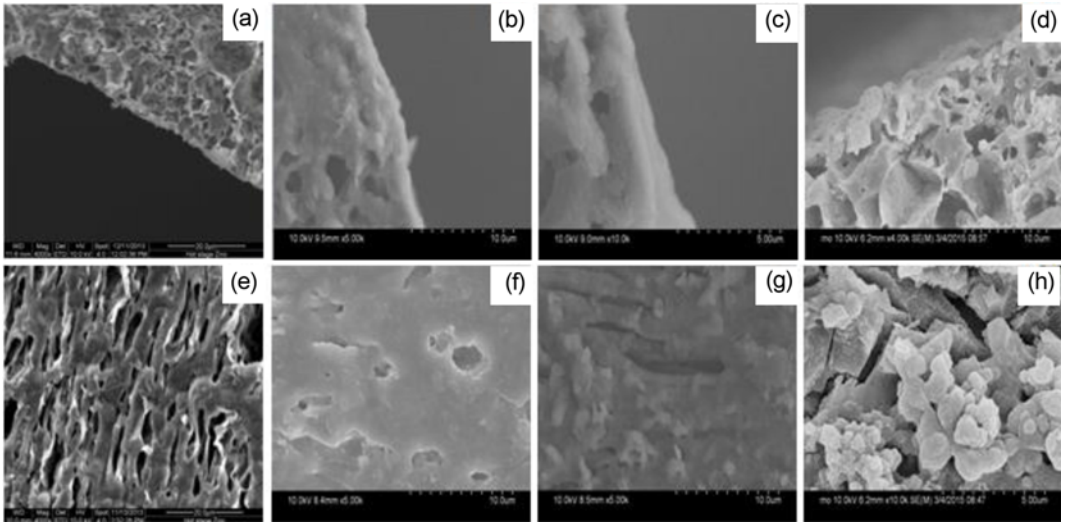

Figure 2. SEM images of the membranes. Cross sectional and surface images of PVDF support membrane ((a) & (e)), PVA coated membrane ((b) & (f)), PVDF/Cu-BTC membrane ((c) & (g)), PVDF/Cu-BTC/2 membrane ((d) & (h)).

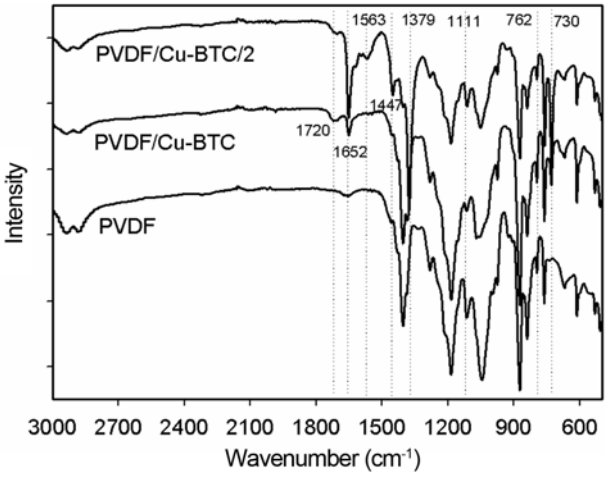

Figure 3. FTIR spectra of the membranes.

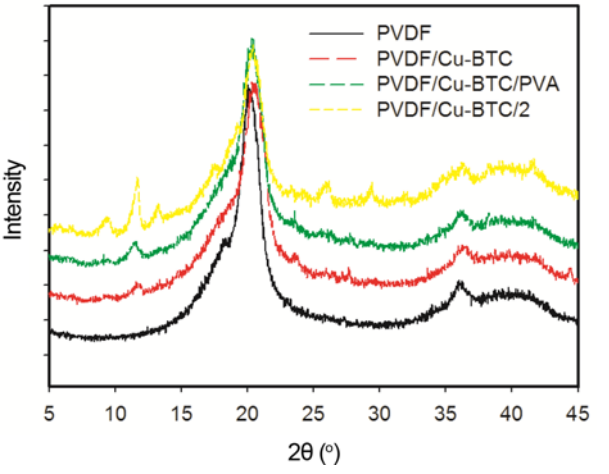

Figure 4. XRD patterns of the membranes.

IR spectra of the membranes are shown in Figure 3. All Membranes had a weak absorption peak at 1652 cm^{-1}, which corresponds to adsorbed water molecules in the incompletely dried PVDF membrane [15]. A peak at around 1720 cm^{-1} (related to the carboxylate ligands) was the emblem of coordination of BTC to the copper site. A peak located at 1563 cm^{-1} was due to the asymmetric stretching vibration of carboxyl in the carbonyl group. The peaks observed at 1447 cm^{-1} and 1379 cm^{-1} corresponded to the symmetric stretching vibration of the carboxyl group of the carbonyl absorption peak. The stretching vibration of C-O-Cu was observed at 1111 cm^{-1}, and the absorption peaks at 762 cm^{-1} and 730 cm^{-1} indicated that groups connected to the benzene ring were replaced by Cu, which are considered to be a characteristic absorption peak for Cu-BTC [16].

Figure 4 shows the XRD patterns of the coated membranes. A typical diffraction of PVDF is found at a 2θ of 19.8° [17,18]. The PVDF/Cu-BTC/2 membrane had peaks at 2θ of 6.8°, 9.5°, 11.5°, and 13.4°, which are related to characteristics of the Cu-BTC crystals. However, the PVDF/Cu-BTC and the PVDF/Cu-BTC/PVA membranes showed much lower intensity of those peaks and no peak 2θ of 6.8° was observed, due to the low crystallinity of the Cu-BTC (Figure 2(g)) [19].

Performance of the Membranes

Table 1 lists the water flux of the Congo Red solution over time for different membranes. The water flux of the PVDF, the PVDF/PVA, and the PVDF/Cu-BTC membranes decreased more than 40 % after 3 h of filtration. This decrease can be attributed to the high hydrophobicity of the PVDF membrane. Congo Red molecules tend to attach to the surface of

Table 1. Flux of the membranes varied with time

Membrane type	Flux (l/m^2h)				
	1 h	2 h	3 h	4 h	Decrease rate (%)
PVDF	127.4	84.9	76.4	76.4	40.0
PVDF/PVA	49.8	33.2	26.5	26.5	46.8
PVDF/Cu-BTC	130.4	101.4	64.0	70.0	46.3
PVDF/Cu-BTC/PVA	33.6	27.8	27.8	27.8	20.9
PVDF/Cu-BTC/2	74.3	64.8	64.8	64.8	12.8

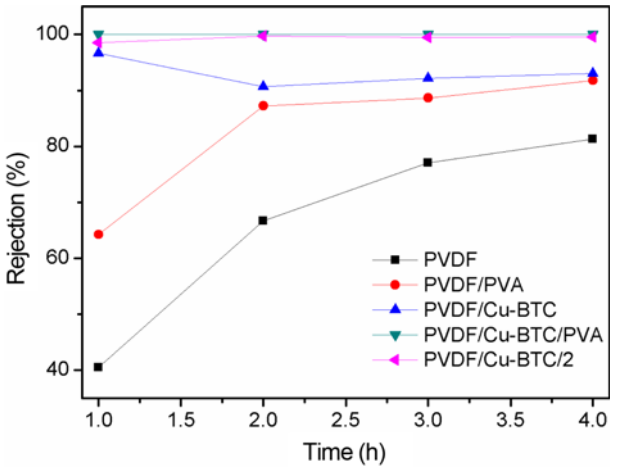

Figure 5. Rejection to Congo Red of the membranes.

hydrophobic membranes, which caused a decrease in the flux. When hydrophilic PVA and Cu-BTC was used, the PVDF/PVA and PVDF/Cu-BTC membranes still had a high decrease in flux due to formation of defects (Figure 2) and an incomplete coverage of the PVDF membranes. On the contrary, the PVDF/Cu-BTC/PVA and PVDF/Cu-BTC/2 membranes showed less decrease in flux than their counterparts in terms of formation of hydrophilic and dense layers. Moreover, the water flux of the dual coated membranes reached a stable value faster than the single coated membranes.

It was found that all composite membranes showed no rejection to the monovalent salt (NaCl) and the divalent salt (Na_2SO_4) used. These two salts are widely used in the dye industry for the crystallization of dyes from solution. Rejection to Congo Red is shown in Figure 5. The PVDF, PVDF/PVA, and PVDF/Cu-BTC membranes did not reject Congo Red completely, although the single coated membranes showed a higher rejection than the pristine PVDF membrane. Rejection of the PVDF and PVDF/PVA membranes increased with filtration time due to the accumulation of Congo Red on the membrane surface. In the case of the PVDF/Cu-BTC membrane, we believe that the rejection decreased with time probably due to damage of the coated Cu-BTC layer in the Congo Red solution. The single layer Cu-BTC formed on the PVDF support degraded very easily due to its imperfect

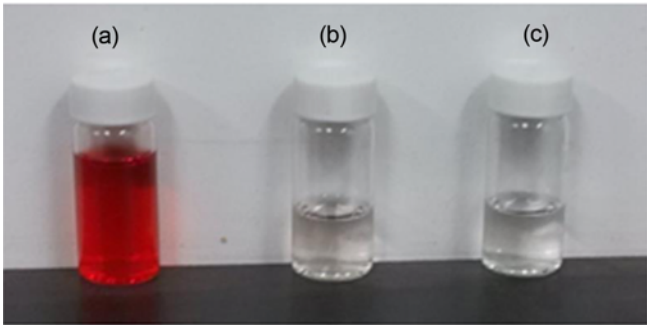

Figure 6. Photos of Congo Red solutions; (a) original solution, (b) permeate in 1 h, and (c) permeate in 4 h.

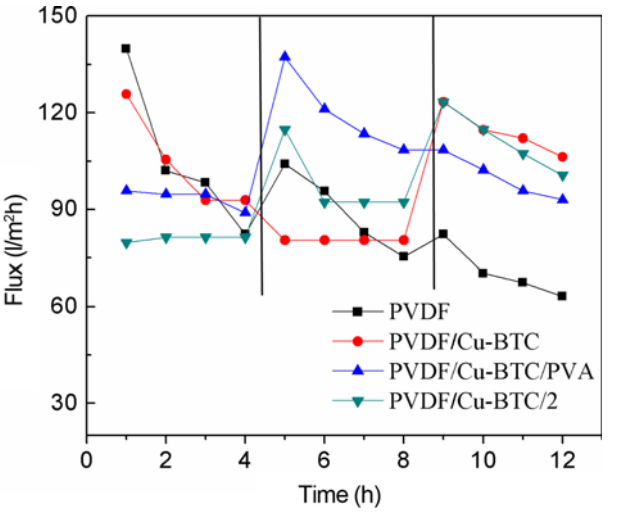

Figure 7. Flux changes of the membranes after continuously filtration for 3 days.

crystallization. Thus, a second synthesis or a PVA coat to protect the formed MOF layer was found to be a critical step. The dual coated membranes (PVDF/Cu-BTC/PVA and PVDF/Cu-BTC/2) showed complete rejection to Congo Red which remained stable during the filtration time. The permeate solution collected for 60 min after 4 h of filtration is shown in Figure 6, a clear solution was observed.

Stability of the membranes being used for the filtration of Congo Red for 3 days is shown in Figure 7. The flux of the PVDF support membrane gradually decreased, even though it was immersed in pure water after each day. Adsorbed Congo Red could not be removed from the membrane by simply immersing it in water. The flux of the PVDF/Cu-BTC membrane also decreased in the first 4 h due to the incomplete covering of the support membrane by Cu-BTC. In the second day, the flux reached a platform after all the pores were covered by Congo Red. On the contrary, the flux of the PVDF/Cu-BTC/PVA and the PVDF/CU-BTC/2 membranes remained stable in the first 4 h per, and then increased after each immersion in pure water. This can be

Table 2. Comparison of dye-salt separation performance of different membranes

Membrane	Water flux l/m^2h @ 0.5 MPa	Rejection to dye (Congo Red) %	Rejection to salts (Na_2SO_4) %	Ref
PVDF/Cu-BTC/2	64.8	>99.5	<1	This study
Cellulose acetate	40.6	>99.0	81	20
PVDF/ZIF8	20.0	>99.0	<1	21

attributed to (1) the ease of removal of the Congo Red when using hydrophilic composite membranes (Cu-BTC and PVA), and (2) the degradation of the Cu-BTC in water. From these results, we can conclude that the composite membranes with Cu-BTC were not suitable for processing aqueous solutions, even after being covered by dual layers of Cu-BTC or PVA.

Table 2 shows that the PVDF/Cu-BTC/2 membrane had a high water flux and an excellent performance in the dye-salt separation in comparison with the cellulose acetate membrane [20] and the PVDF/ZIF8 membrane [21]. The cellulose membrane had a reasonable water flux and a high rejection to Congo Red, however, it also retained salts. The PVDF/ZIF8 membrane showed a similar performance to the PVDF/Cu-BTC/2 membrane in the dye-salt separation, but had a much lower water flux due to the hydrophobicity of the ZIF8.

Conclusion

In summary, PVDF/Cu-BTC composite membranes were fabricated by *in situ* formation of Cu-BTC frameworks on PVDF hollow fiber support membranes. A PVA coating layer was used to protect the MOF layer from degradation in aqueous solution. FTIR, XRD, and SEM characterization showed that the Cu-BTC MOF structure was successfully formed on the surface of the membrane. It was noticed that the composite membranes showed no rejection to divalent salts, but high rejection of Congo Red molecules. It was demonstrated that the polymer-MOF composite membranes displayed promising application in the separation of dye solutions. However, the Cu-BTC structure was instable in aqueous solution even with a PVA layer coating on its surface. A more stable MOF material in aqueous solution should be developed on a polymeric support for better performance in dye separation.

Acknowledgements

The authors acknowledge the financial support from the National Natural Science Foundation of China (Grants No. 51373119), National Key Basic Research Development Program (973 Program) (No. 2014CB660813), and Science and Technology Plans of Tianjin (No. 16YFZCSF00330, 15PTSYJC00250).

References

1. S. Yu, C. Gao, H. Su, and M. Liu, *Desalination*, **140**, 97 (2001).
2. W. J. Lau and A. F. Ismail, *Desalination,* **245**, 321 (2009).
3. I. Koyuncu and D. Topacik, *J. Membr. Sci.,* **195**, 247 (2002).
4. J. Lin, W. Ye, M.-C. Baltaru, Y. P. Tang, N. J. Bernstein, P. Gao, S. Balta, M. Vlad, A. Volodin, A. Sotto, P. Luis, A. L. Zydney, and B. V. der Bruggen, *J. Membr. Sci.,* **514**, 217 (2016).
5. Y. He, G.-M. Li, H. Wang, Z.-W. Jiang, J.-F. Zhao, H.-X. Su, and Q.-Y. Huang, *J. Taiwan Inst. Chem. Eng.*, **40**, 289 (2009).
6. P. Banerjee, S. DasGupta, and S. De, *J. Hazar. Mater.*, **140**, 95 (2007).
7. L.-F. Fang, N.-C. Wang, M. Zhou, B. Zhu, L. Zhu, and A. E. John, *Chinese J. Polym. Sci.*, **33**, 1491 (2015).
8. S. K. Maurya, K. Parashuram, P. S. Singh, P. Ray, and A. V. R. Reddy, *Desalination*, **304**, 11 (2012).
9. X. Li, Y. Chen, X. Hu, Y. Zhang, and L. Hu, *J. Membr. Sci.*, **471**, 118 (2014).
10. S. Wang and Y. Peng, *Chem. Eng. J.*, **156**, 11 (2010).
11. L. S. Chan, W. H. Cheung, S. J. Allen, and G. Mckay, *Sep. Purif. Tech.*, **67**, 166 (2009).
12. B.-J. Yao, W.-L. Jiang, Y. Dong, Z.-X. Liu, and Y. B. Dong, *Chem. Eur. J.,* **22**, 1 (2016).
13. X.-S. Wang, J. Liang, L. Li, Z.-J. Lin, P. P. Bag, S.-Y. Gao, Y.-B. Huang, and R. Cao, *Inorg. Chem.,* **55**, 2641 (2016).
14. X. Zhao, S. Liu, Z. Tang, H. Niu, Y. Cai, W. Meng, F. Wu, and J. P. Giesy, *Sci. Rep*., **5**, 11849 (2015).
15. S. Srisude and B. Virote, *J. Environ. Sci.*, **20**, 379 (2008).
16. J. Hu, H. Cai, H. Ren, Y. Wei, Z. Xu, H. Liu, and Y. Hu, *Ind. Eng. Chem. Res.*, **49**, 12605 (2010).
17. Y. Chen, J. Guo, and H. Kim, *Reac. Funct. Polym.*, **70**, 69 (2010).
18. X. Ren and Y. Dzenis, *Mater. Res. Soc. Sympos. Proc.*, doi:10.1557/PROC-0920-s03-03 (2006).
19. Y.-K. Seo, G. Hundal, I. T. Jang, Y. K. Hwang, C.-H. Jun, and J.-S. Chang, *Microporous Mesoporous Mat.*, **119**, 331 (2009).
20. Y. He, G.-M. Li, H. Wang, Z.-W. Jiang, J.-F. Zhao, H.-X. Su, and Q.-Y. Huang, *J. Taiwan Inst. Chem. Eng.*, **40**, 289 (2009).
21. S. F. Zhang, Master Thesis, Tianjin Polytechnic University, 2015.